ARTICLE

Biallelic *USP14* variants cause a syndromic neurodevelopmental disorder

Frédéric Ebstein[1,2],*, Xenia Latypova[3], Ka Ying Sharon Hung[4], Miguel A. Prado[4,5], Byung-Hoon Lee[4,6], Sophie Möller[1], Martin Wendlandt[1], Barbara A. Zieba[1], Laëtitia Florenceau[2], Virginie Vignard[2,3], Léa Poirier[2], Bérénice Toutain[2], Isabella Moroni[7], Charlotte Dubucs[8,9], Nicolas Chassaing[9], Judit Horvath[10], Holger Prokisch[11,12], Sébastien Küry[2,3], Stéphane Bézieau[2,3], Joao A. Paulo[4], Daniel Finley[4], Elke Krüger[1], Daniele Ghezzi[13,14], Bertrand Isidor[2,3],*

A B S T R A C T

Purpose: Imbalances in protein homeostasis affect human brain development, with the ubiquitin-proteasome system (UPS) and autophagy playing crucial roles in neurodevelopmental disorders (NDD). This study explores the impact of biallelic *USP14* variants on neurodevelopment, focusing on its role as a key hub connecting UPS and autophagy.

Methods: Here, we identified biallelic *USP14* variants in 4 individuals from 3 unrelated families: 1 fetus, a newborn with a syndromic NDD and 2 siblings affected by a progressive neurological disease. Specifically, the 2 siblings from the latter family carried 2 compound heterozygous variants c.8T>C p.(Leu3Pro) and c.988C>T p.(Arg330*), whereas the fetus had a homozygous frameshift c.899_902del p.(Lys300Serfs*24) variant, and the newborn patient harbored a homozygous frameshift c.233_236del p.(Leu78Glnfs*11) variant. Functional studies were conducted using sodium dodecyl-sulfate polyacrylamide gel electrophoresis, western blotting, and mass spectrometry analyses in both patient-derived and CRISPR-Cas9-generated cells.

Results: Our investigations indicated that the *USP14* variants correlated with reduced N-terminal methionine excision, along with profound alterations in proteasome, autophagy, and mitophagy activities.

Conclusion: Biallelic *USP14* variants in NDD patients perturbed protein degradation pathways, potentially contributing to disorder etiology. Altered UPS, autophagy, and mitophagy activities underscore the intricate interplay, elucidating their significance in maintaining proper protein homeostasis during brain development.

*Correspondence and requests for materials should be addressed to Frédéric Ebstein, National Institute of Health and Medical Research, L'institut du thorax, IRS-UN - 8 quai Moncousu - BP 70721, Nantes 44007, France. *Email address:* frederic.ebstein@univ-nantes.fr OR Bertrand Isidor, Nantes Université, CHU Nantes, Service de Génétique Médicale, Nantes 44000, France. *Email address:* bertrand.isidor@chu-nantes.fr
Affiliations are at the end of the document.

Introduction

A tight regulation of protein homeostasis is crucial to vertebrate neurodevelopment. In eukaryotic cells, the ubiquitin-proteasome system (UPS) and autophagy participate in maintaining the highly dynamic pool of intracellular proteins by preferentially eliminating damaged or mutant proteins.[1] Ubiquitination is a central post-translational modification (PTM) process that mediates the covalent tagging of protein substrates destined for recognition and subsequent degradation by the proteasome and autophagy. Depending in part on ubiquitin chain topology, ubiquitin-modified substrates may indeed be targeted to the 26S proteasome or LC3-positive autophagosomes. Importantly, once proteasome substrates have been committed to degradation, ubiquitin must be removed to facilitate substrate unfolding and subsequent translocation into the 20S catalytic core particle.[2] There exist three proteasome-associated deubiquitinating enzymes (DUB) capable of trimming ubiquitin chains from protein substrates before their degradation, namely, the 2 cysteine proteases USP14[3] (Ub-specific protease 14, Ubp6 in *Saccharomyces cerevisiae*) and UCH37/UCHL5,[4] as well as the metalloprotease PSMD14 (Rpn11).[5] In addition to cleaving ubiquitin from protein substrates, USP14 and its yeast ortholog Ubp6 have been shown to regulate proteasome activity via both their catalytic domains and their N-terminal ubiquitin-like (UBL) domains.[6] Moreover, USP14 exhibits multiple regulatory roles, such as the modulation of GABAergic synapses,[7] as well as negative feedback between UPS and autophagy.[8] USP14 is thus a cellular pivot orchestrating the cross talk between these 2 proteolytic pathways.

Proper functioning of the UPS is essential to neurodevelopment because several critical signaling pathways involved in early development of the central nervous system (CNS), such as synaptogenesis, are regulated by ubiquitination.[9] Several DUBs have been associated with impaired neurodevelopment, an observation that is in line with the emerging view that UPS dysfunction is a major pathophysiological mechanism of neurodevelopmental disorders (NDD).[10] These include notably Hao-Fountain syndrome (MIM: 602519), which is caused by *USP7* dominant variants.[11] Variants of the *USP9X* (MIM: 300072) and *USP27X* (MIM: 300975) genes are also a common cause of either X-linked dominant (MIM: 300968)[12] or recessive NDD (MIM: 300919, XLID105).[13,14] Similarly, variants in genes coding for DUBs such as *EIF3F* (MIM: 618295),[15] *STAMBP* (MIM: 614261),[16] *ALG13* (MIM: 300884),[17] or *OTUD6B* (MIM: 617452)[18] have been associated with NDD. In this study, we provide evidence that biallelic *USP14* variants are responsible for severe neurodevelopmental syndrome and explore the functional consequences of *USP14* impairment.

Materials and Methods

Ethics statement

Human genetic studies conducted in research laboratories were approved by local ethics committees from participating centers. Written informed consent was obtained for all individuals of the study by their parents before testing. All affected individuals underwent clinical examination by at least 1 expert clinical geneticist of each center.

Exome sequencing

For exome sequencing (ES), DNA was extracted from peripheral blood mononuclear cells (PBMC). We performed ES within diagnostic or research settings according to manufacturer's instructions, generated and aligned to human genome hg19 assembly. ES data analysis was performed following Genome Analysis Toolkit's best practices (v3.4).

Generation of CRISPR/Cas9 *USP14* knockout clones

A guide RNA sequence (CTCTACTCCGGTGAGCCCTGCG GTG) targeting the first exon of the *USP14* gene was cloned into the pSpCas9(BB)-2A-Puro (PX459, V2.0, Addgene, #62988) using the BbsI restriction sites. The Cas9 expression vector containing the guide RNA was introduced into SH-SY5Y cells using the JetPRIME transfection reagent (Polyplus-transfection SA) following the manufacturer's recommendations. At 24-hour after transfection, cells were plated at low density in 96-well plates in the presence of puromycin (10 μg/ml). Resistant clones were further cultivated and assessed for *USP14* exon 1 damages by polymerase chain reaction (PCR) amplification before Sanger sequencing.

Cell culture

PBMC collected from patients carrying *UPS14* variants (individuals 1 and 2) and related healthy individuals were subjected to T cell expansion by seeding them on irradiated feeder cells in the presence of IL-2 (50 U/ml) and L-PHA (1 mg/ml) for 3 to 4 weeks. The SH-SY5Y neuroblastoma cell line was a laboratory stock cultivated in the presence of Dulbecco's Modified Eagle medium supplemented with 10% fetal bovine serum and 1% penicillin/streptomycin. After obtaining informed consent, skin biopsies were obtained from individual of family 1 following standard clinical procedure. Fibroblast cell lines were cultured in DMEM medium supplemented with 10% fetal bovine serum, 1 mM sodium pyruvate, 4 mM glutamine, and 1% penicillin/ streptomycin.

SDS-PAGE and western blotting

Cells were lysed in standard radioimmunoprecipitation assay buffer (50 mM Tris pH 7.5, 150 mM NaCl, 2 mM EDTA, 1% NP40, 0.1% SDS), and proteins were quantified by bicinchoninic acid assay following the manufacturer's instructions. Ten to 20 μg of protein lysates were separated by 10%, 12%, or 15% sodium dodecyl-sulfate polyacrylamide gel electrophoresis (SDS-PAGE) and subsequently blotted (200V, 400 mA, 1 hour) onto

polyvinylidene difluoride membranes (Millipore). Primary antibodies used in this study were directed against USP14 (Santa Cruz Biotechnology Inc, clone F4), α4 proteasome subunit (ie, PSMA7, Enzo Life Sciences, clone MCP34), BNIP3L (Cell Signaling Technology, 12396), LC3B (Cell Signaling Technology, 3868), β5 (ie, PSMB5) proteasome subunit (Abcam, ab3330), Rpt1 (ie, PSMC2) proteasome subunit (Enzo Life Sciences, BML-PW8315), α-tubulin (Abcam, DM1A), and GAPDH (Cell Signaling Technology, clone 14C10). After overnight incubation, membranes were incubated with anti-mouse- and anti-rabbit-conjugated secondary antibodies (1/5000) for 1 hour at room temperature. Proteins were visualized using Clarity Western electrochemiluminescence Substrate (Biorad).

In-plate peptidase activity assay

Cells were lysed in ice-cold homogenization TSDG buffer (10 mM Tris pH 7.0, 10 mM NaCl, 25 mM KCl, 1.1 mM MgCl$_2$, 0.1 mM EDTA, 2 mM dithiothreitol (DTT), 2 mM ATP, 1 mM NaN$_3$, 20 % glycerol) and proteins were extracted using freeze/thawing in liquid nitrogen. Protein quantification of the soluble lysates was determined by Bradford. Proteasome chymotrypsin-like activity was measured on 96-well opaque microtiter plates (Greiner) by incubating 10 μg of TSDG-generated whole-cell lysates with 0.1 mM of the Suc-Leu-Leu-Val-Tyr-7-amino-4-methylcoumarin (AMC) proteasome fluorogenic peptide (Bachem) in quadruplicates in a final volume of 100 μl. AMC release was measured over a 3-hour period of time using a fluorescence plate reader at 360/460 nm (NanoQuant Plate, Tecan).

RNA extraction and reverse transcription-qPCR

Total RNA was isolated from resting T cells using the kit from Analytic Jena AG following the manufacturer's instructions. Isolated RNA (100-500 ng) was next reverse transcribed using the M-MLV reverse transcriptase (Promega) following the manufacturer's recommendations. Quantitative PCR (qPCR) was performed using the Premix Ex Taq (probe qPCR purchased from TaKaRa) and in duplicates to determine the messenger RNA (mRNA) levels of 6 interferon (IFN)-stimulated genes (ISG) using FAM-tagged TaqMan Gene Expression Assays obtained from Thermo Fisher Scientific according to the manufacturer's instructions. TaqMan probes used in this study for ISG quantification included IFI27, IFI44L, IFIT1, ISG15, RSAD2, and SIGLEC1. The cycle threshold (Ct) values for target genes were converted to values of relative expression using the relative quantification method ($2^{-\Delta\Delta Ct}$). Target gene expression was calculated relative to Ct values for the GAPDH control housekeeping gene. A type I IFN score representing the median fold change of the 6 ISG relative to a single calibrator control was calculated for each sample.

Plasmid construction and transfection

The cDNA for *USP14* was amplified by RT-qPCR from total RNA isolated from SH-SY5Y neuroblastoma cells and cloned into the pcDNA3.1/*myc*-polyhistidine (HIS) expression vector (Invitrogen). The single-amino-acid substitutions p.(Leu3Pro) and p.(Arg330*) were introduced by site-directed mutagenesis and inverse PCR, respectively. SH-SY5Y wild-type (WT) and *USP14* knockout cells were transfected using JetPRIME reagent (Polyplus-transfection SA) according to the instructions of the manufacturer.

Purification of USP14 and proteasome

Human *USP14* WT and p.(Leu3Pro) were subcloned into the pET small ubiquitin-related modifier (SUMO) TA vector (Invitrogen), then transferred into the pTXB1 vector (NEB) for N-terminal His-SUMO and C-terminal intein/chitin binding domain (CBD) tagging. The constructs were expressed in *E. coli* Rosetta 2 (DE3) cells (Novagen) and purified using Ni-NTA agarose resin (Qiagen) according to the manufacturer's instructions. The His-SUMO tag was cleaved using the His-Ulp1 SUMO protease, and the resulting USP14-intein-CBD protein was retrieved on Ni-NTA resin. USP14-intein-CBD, WT or p.(Leu3Pro), was further purified on chitin beads and released from the beads in untagged form by DTT cleavage. Human proteasomes were affinity purified as previously described[19] from a stably transformed HEK293T cell line in which proteasome subunit Rpn11 is Histidine-TEV-Biotin-Histidine-tagged. This tag induces biotinylation, and proteasomes were thus isolated from the lysate using NeutrAvidin agarose resin (Thermo Scientific). The proteasome was eluted from the resin by tobacco etch virus cleavage, which removes the Histidine-TEV-Biotin-Histidine tag. Ubiquitin-vinylsulfone (Ub-VS)-treated proteasome was prepared by on-column incubation with 2.5 μM Ub-VS before tobacco etch virus cleavage.

In vitro deubiquitination and degradation assays

To compare the deubiquitinating activity of the proteasome-free form of WT or p.(Leu3Pro) USP14, each variant was tested at 1.5 μM by incubating with subsaturating amounts of ubiquitin-amido methyl coumarin (Ub-AMC; 1.5 μM) in an assay buffer of 50 mM Tris-HCl (pH 7.5), 1 mM EDTA, 1 mM ATP, 5 mM MgCl$_2$, 1 mM DTT, and 1 mg/mL ovalbumin. To measure proteasome-bound USP14 activity for kinetic analysis, 1 nM Ub-VS-treated human proteasomes was reconstituted with graded concentrations of recombinant USP14 and 1 μM Ub-AMC. Ub-AMC cleavage was monitored in real time by measuring fluorescence at Ex365/Em460 with an Envision Plate reader (Perkin Elmer) equipped with an appropriate mirror (eg, LANCE/DELFIA, 400 nm). To perform in vitro deubiquitination and degradation assays with ubiquitin conjugates as the physiological

substrate, 4 nM human proteasome was incubated with polyubiquitinated N-terminal cyclin B1 (Ub$_n$NCB1; ~120 nM final; hemagglutinin-tagged) or polyubiquitinated full-length cyclin B1 (Ub$_n$CCNB1; ~40 nM final) in proteasome assay buffer (50 mM Tris-HCl [pH 7.5], 5 mM MgCl$_2$, 5 mM ATP). Purified recombinant USP14 WT or p.(Leu3Pro) was reconstituted with proteasome for 5 minutes before initiating the reaction. Reactions were quenched by adding 5 × SDS-PAGE sample buffer, boiled for 5 minutes, then subjected to SDS-PAGE and immunoblotting analysis using anti-HA-horseradish peroxidase (Roche) or anti-cyclin B1 (Neomarkers) antibody.

Mass spectrometry (MS) analysis

In-gel protein digestion with trypsin was performed on SDS-PAGE loaded with 10 µg of whole-cell lysates generated from fibroblasts of 1 heathy donor, as well as individuals carrying single or biallelic *USP14* variants. The resulting digested peptides were extracted from the gel, and a mixture of heavy-labeled peptides containing 20 fmol of both WT (PLYSVTVK) and p.(Leu3Pro) (PPYSVTVK) USP14 peptides was added. Both peptides were labeled with a heavy valine [13C(5)15N(1), +6 Da]. Subsequently, peptides were then desalted and analyzed on a Q-Exactive MS instrument (Thermo Scientific) using a PRM (parallel reaction monitoring) method to monitor the abundance of the labeled light and heavy peptides used for quantification. Specifically, the heavy-labeled standards were used for quantifying endogenous WT and p.(Leu3Pro) peptides in all samples through an Absolute QUAntification (AQUA) MS-based method, as previously described.[20]

Results

Clinical features of individuals with biallelic *USP14* variants

Here, we describe the phenotypic features of 4 individuals from 3 unrelated families (Table 1, Supplemental Figure 1). We identified 2 *USP14* variants in 2 affected individuals of family 1 and submitted our data to GeneMatcher platform[21] from which patients 3 and 4 were further enlisted. The 2 patients from family 1 showed a progressive neurological disease with onset in the first 2 years of life, characterized by ptosis, nystagmus, tongue fasciculations, proximal upper and lower limb muscular weakness, hand tremor, and dysmetria. The clinical course was relentless progressive with early wheelchair need: in the last neurological examination at the age of 16 and 18 years, both siblings had developed optic neuropathy, multiple tendon retractions, and severe scoliosis requiring surgery. No specific scales were used for scoring neurological severity. Cognitive functions, assessed with the Wechsler Intelligence Scale for Children and the Wechsler Adult Intelligence Scale, remained unaffected.

Individual 3 from family 2 is a male fetus from consanguineous parents examined after a premature termination of pregnancy at 29 weeks and 4 days of gestation. Prenatal follow-up detected intrauterine growth restriction. Brain examination showed lissencephaly, corpus callosum agenesis, aqueductal stenosis, and ventricular dilation. Hypospadias was also observed, and limb examination revealed bilateral clinodactyly, bilateral adducted thumbs, a bilateral unique palmar fold, and bilateral equinovarus feet.

Individual 4 from family 3, born to consanguineous parents, died on the second day of life. Autopsy revealed pachygyria, hydrocephalus, and corpus callosum agenesis. He presented with hip dislocation, hepatomegaly, and Fallot tetralogy. Extremities examination showed bilateral post axial hands hexadactyly and multiple congenital contractures.

Genetic variations

Individuals 1 and 2 carried 2 heterozygous variants in *USP14* (NM_005151.4), namely, a c.988C>T p.(Arg330*) nonsense variant leading to premature protein truncation, and a non-synonymous c.8T>C p.(Leu3Pro) variant (Figure 1A, Supplemental Figure 1). Familial segregation study confirmed that each variant was inherited from 1 of the unaffected parents. Both variants were absent in gnomAD[22] (v3.1 accessed on July 21th, 2023). The c.8T>C p.(Leu3Pro) variant, located within the first exon of *USP14* (Figure 1B), was predicted as deleterious by in silico bioinformatic tool combined annotation dependent depletion v1.4:.22.4. Importantly, Leu3 is a highly conserved USP14 residue across species and located at the N terminus of USP14's UBL domain (Figure 1B and C), which is involved in proteasome association.[23]

A homozygous c.899_902del p.(Lys300Serfs*24) *USP14* variant, with a gnomAD frequency $f = 0.00000796$ (2 heterozygous individuals in gnomAD exomes) was found in individual 3 from family 2 (Supplemental Figure 1). Individual 4 from family 4 carried a homozygous c.233_236del p.(Leu78Glnfs*11) *USP14* variant, which was absent in gnomAD. In families 2 and 3, the variants were detected as heterozygous in each asymptomatic parent (Supplemental Figure 1). According to the American College of Medical Genetics and Genomics and Association for Molecular Pathology criteria,[24] c.8T>C is classified as variant of uncertain significance (VUS, PM2), c.988C>T and c.899_902del c.233_236del as likely pathogenic (PVS1 and PM2) and c.233_236del as pathogenic (PVS1, PM2, and PP5).

Functional consequences of *USP14* variants

### Impact of *USP14* variants on proteasome activity

Considering the ability of USP14 to inhibit proteasome activity allosterically,[6] we first sought to determine the impact of the p.(Arg330*) and p.(Leu3Pro) *USP14* variants

Table 1 Clinical features of the patients with nonsense, missense and copy number variants involving *USP14*

Family	Family 1	Family 1	Family 2	Family 3	Turgut et al, 2021	Turgut et al, 2021	Turgut et al, 2021
Individual	P1	P2	P3	P4	P6 – Fetus 1	P6 – Fetus 2	P6 – Fetus 3
Variant type	Compound heterozygous missense + nonsense	Compound heterozygous missense + nonsense	Homozygous frameshift	Homozygous frameshift	Homozygous frameshift	Homozygous frameshift	Homozygous frameshift
Variant (NM_005151.4)	c.8T>C p.(Leu3Pro) and c.988C>T p.(Arg330*)	c.8T>C p.(Leu3Pro) and c.988C>T p.(Arg330*)	c.899_902del p.(Lys300Serfs*24)	c.233_236del p.(Leu78Glnfs*11)	c.233_236del p.(Leu78Glnfs*11)	c.233_236del p.(Leu78Glnfs*11)	c.233_236del p.(Leu78Glnfs*11)
Gender	M	F	M	ND	M	M	M
Age at last follow up	18 y	16 y	NA	2 days	NA	NA	NA
Birth term (WG)	38	38	PTP 29+4 weeks of gestation	Premature birth at 29 weeks of gestation	PTP at 27 weeks of gestation	PTP at 20 weeks of gestation	PTP at 21+4 weeks of gestation
Pregnancy complications	–	–	NA	–	Polyhydramnios	Polyhydramnios	Hydramnios
Birth weight (grams/SD)	4020	2840	1224	ND	950 (−0.3 SD)	380	460
Birth length (cm/SD)	ND	48	34	ND	30 (−2.43 SD)	25	25
OFC at birth (cm/SD)	ND	34	27	ND	24.5 (−0.47 SD)	19	19.5
DD/ID	+	+	NA	NA	NA	NA	NA
Hypotonia	–	–	NA	NA	NA	NA	NA
Speech impairment	+	+	NA	NA	NA	NA	NA
Abnormal brain imaging	–	–	+	+	NA	+	+
Congenital malformations/ additional findings	Severe scoliosis (surgery at 17 y)	Severe scoliosis (surgery at 15 y)	Hypospadias	VSD, Fallot	No	No	No
Abnormal extremities	–	–	+	+	+	+	+
Ophthalmological findings	Optic neuropathy	Optic neuropathy	NA	NA	NA	NA	NA
Dysmorphic features	+	+	+	ND	+	+	+

DD/ID, developmental delay/intellectual disability; *F*, female; *M*, male; *ND*, not determined; *OFC*, occipital frontal circumference; *PTP*, premature termination of pregnancy; *SD*, standard deviation; *VSD*, ventricular septal defect.
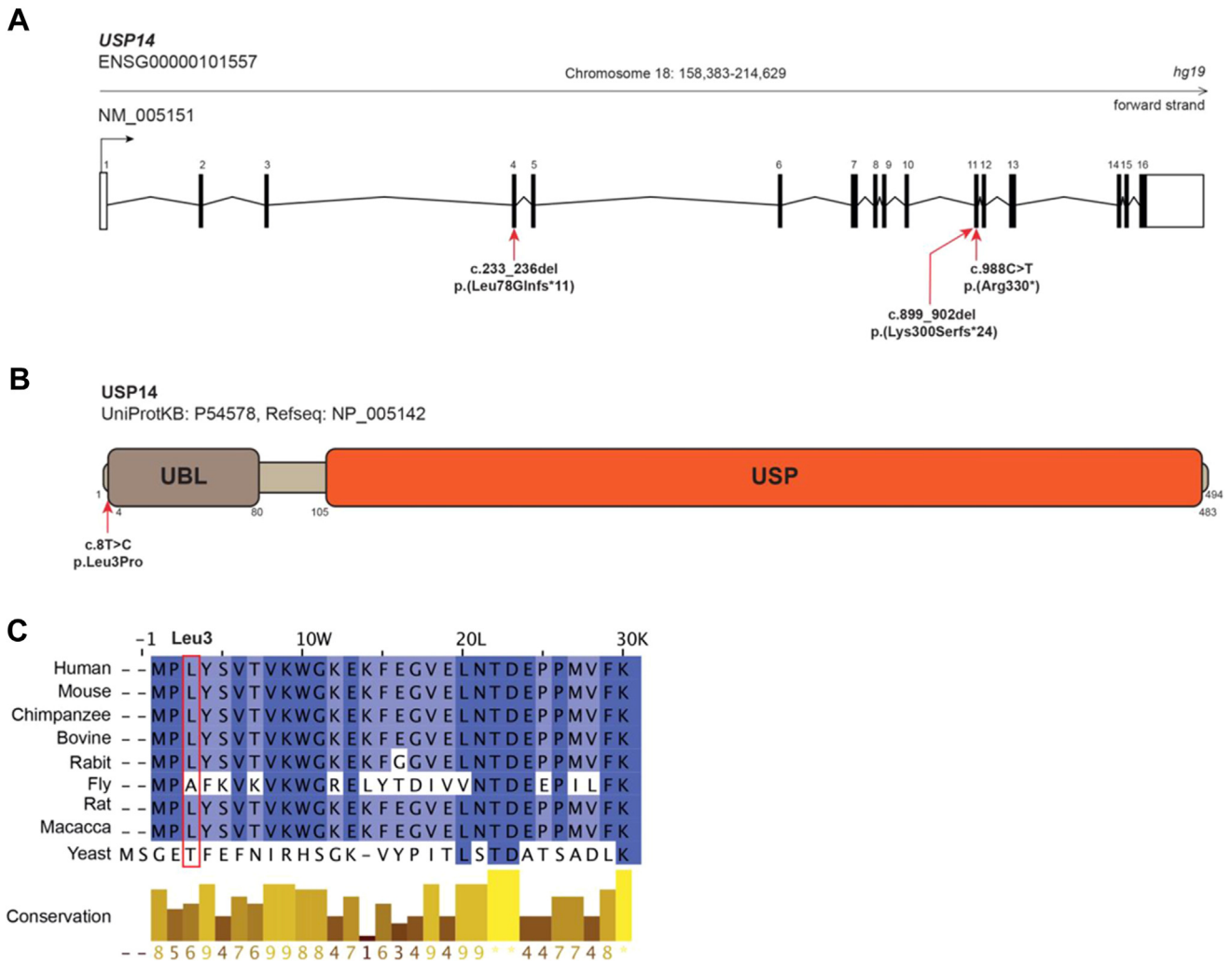
Figure 1 *USP14* **variants.** A. Exon structure of longest *USP14* transcript, containing 16 exons (NM_005151). Nonsense and frameshift variants identified in the present study are indicated with red arrows. B. Protein structure of USP14 (UniProtKB - P54578). Functional domains (PROSITEannotation rule, UniProtKB/Swiss-Prot format) are indicated. UBL, ubiquitin-like domain; USP, ubiquitin-specific protease domain. Nonsynonymous variant c.8T>C p.(Leu3Pro); (individuals 1 and 2) is indicated with a red arrow. C. Multiple sequence alignment of USP14 orthologs from 8 eukaryotic species compared with USP14 human protein sequence. Clustal W multiple sequence alignment program. Conservation scores are mentioned below the alignment. Red boxes identify variant positions.

on proteasome function. To this end, T cells from both affected siblings, as well as their parents, were assessed for their capacity to cleave the Succinyl-Leu-Leu-Val-Tyr-7-amido-4-methylcoumarin proteasome reporter substrate using a previously described in-plate activity assay.[18,25] As shown in Figure 2, the monoallelic and/or biallelic *USP14* variants carried by the family members were all associated with increased proteasome chymotrypsin-like activity when compared with that from a healthy donor control of WT genotype. The observation that both p.(Arg330*) and p.(Leu3Pro) *USP14* variants suppress the described inhibitory properties of USP14 on proteasomes[26] strongly suggests that such alterations are loss-of-function variants. Interestingly, the 2 variants were not equal in their ability to activate proteasomes, with p.(Leu3Pro) being more efficient than p.(Arg330*) in elevating chymotrypsin-like activity in T cells from the father and the 2 siblings (Figure 2).

Effects of *UPS14* variants on USP14 DUB activity

We next examined the impact of the Leu3Pro substitution on the ability of USP14 to remove ubiquitin moieties from protein substrates in vitro. For this purpose, N-terminally SUMO-tagged versions of both WT and p.(Leu3Pro) USP14 proteins were expressed in *E. coli* and subsequently purified after tag cleavage, as previously described.[27] As shown in Figure 3A, no discernible differences could be observed between WT and p.(Leu3Pro) USP14 in their ability to hydrolyze the standard fluorogenic substrate ubiquitin-AMC. Given that USP14 undergoes an ~800-fold activation upon association with the proteasome,[28] we next compared the activity profile of WT and p.(Leu3Pro) USP14 when associated with purified 26S proteasomes. Interestingly, the deubiquitinating activity of recombinant USP14 in this activated state was also not detectably affected by the p.(Leu3Pro) variant. (Figure 3B), suggesting that the
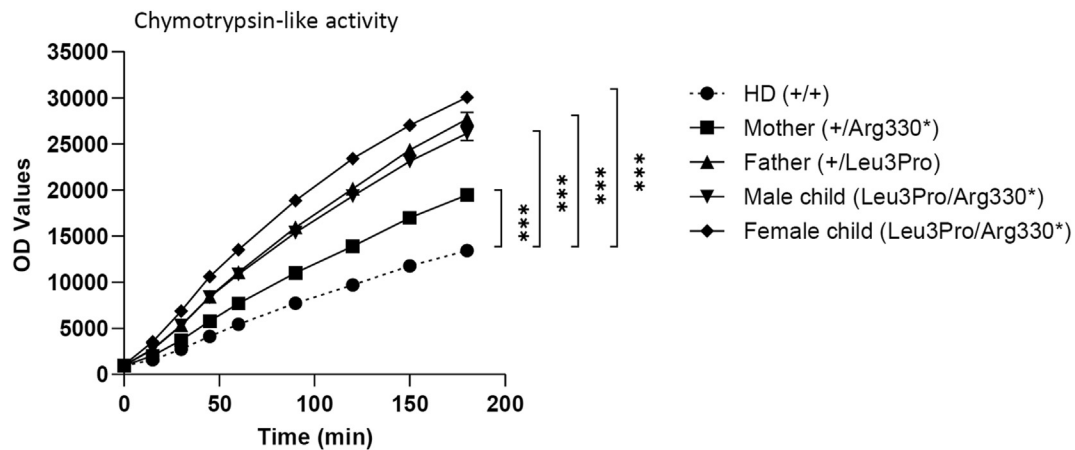
Figure 2 **Subjects with UPS14 variants exhibit increased proteasome activity.** Ten μg of native cell lysates generated from T cells of a healthy donor (HD) and subjects carrying the p.(Arg330*) and/or p.(Leu3Pro) USP14 variants were incubated at 37°C on a 96-well plate in a final 100 μl volume containing 0.1 mM of the Suc-LLVY-AMC fluorogenic peptide. Fluorescence activity reflecting proteasome chymotrypsin-like activity was measured at 360/460 nm on a microplate reader over a 180-minute period of time, as indicated. ***$P < .001$ (unpaired two-tailed t test, $n = 4$).

p.(Leu3Pro) *USP14* variant does not significantly affect the removal of ubiquitin from protein substrates at the proteasome. In agreement with these findings, WT and p.(Leu3Pro) USP14 were capable of trimming ubiquitin chains from the NCB1 (an N-terminal fragment derived from cyclin B1; Figure 3C) and CCNB1 (full-length cyclin B1; Figure 3D) poly-ubiquitinated substrates with comparable efficiencies, as determined by western blotting. Finally, we investigated the activity state of USP14 in fibroblasts isolated from both affected siblings and their mother by performing a DUB labeling experiment using HA-Ub-VS probe, a strong electrophile that reacts with active cysteine residue of USP14 to form a covalent adduct.[28] As shown in Figure 3E, the activity state of the p.(Leu3Pro) *USP14* variant in in proband fibroblasts was similar to that of WT USP14 in maternal fibroblasts. Altogether, these data indicate that the Leu3Pro substitution does not substantially affect USP14 DUB activity.

Influence of USP14 dysfunction on autophagy/mitophagy

Western blot analysis of the T cell samples from the siblings and their parents from family 1 further revealed that the p.(Arg330*) variant was associated with reduced amounts of USP14 full-length protein in the mother, as well as male and female children (Figure 4). It is noteworthy that we were unable to detect the USP14$_{(1-229)}$ truncated protein, which would theoretically arise from the p.(Arg330*) variant and run at the expected size of 36.7 kDa. The inability of the p.(Arg330*) variant to generate a protein product was likely due to the significant reduction in mRNA expression of the c. 988C>T mutant allele compared with that of the c. 988C WT allele (Supplemental Figure 2A). This observation also suggests that USP14 mRNAs carrying the c. 988C>T variant were promptly targeted for nonsense-mediated

mRNA decay (NMD), preventing their translation into proteins. Despite comparable amounts of total USP14 mRNA (Supplemental Figure 2B), the protein levels of the p.(Leu3Pro) *USP14* variant were also slightly diminished in the father's T cells compared with those of WT USP14 in T cells from a healthy donor (Supplemental Figure 3A and B). This suggests that the p.(Leu3Pro) variant may exhibit a higher protein turnover rate than its WT counterpart, despite that proteasome inhibition by bortezomib treatment (although promoting the accumulation of ubiquitin-modified proteins) failed to stabilize all forms of USP14 (Supplemental Figure 3A and B).

Noteworthy, the expression of α4 proteasome subunits did not substantially vary across the 4 samples, indicating that the increased chymotrypsin-like activity triggered by the *USP14* variants did not occur as a consequence of increased proteasome amounts. Because USP14 is a well-known modulator of autophagy,[19] we next monitored the steady-state expression level of the autophagy marker LC3B-II in both parental and progenitor T cells. As shown in Figure 4, our western blot analysis of these samples uncovered that both affected siblings carrying biallelic *UPS14* variants exhibited increased levels of LC3b-II, compared with their parents, suggesting elevated autophagosome formation in the cells of affected individuals. The dysregulated autophagy associated with *USP14* biallelic variants was further accompanied by a severe loss of the mitophagy receptor BNIP3L/NIX (Figure 4), indicating that mitophagy was also perturbed in these samples. Further investigations of these specimens confirmed that *USP14* compound heterozygosity led to increased mitochondrial autophagy flux, as evidenced by decreased expression of the mitochondrial proteins BNIP3 and PINK1 in both affected siblings, compared with their parents (Supplemental Figure 4A and B).
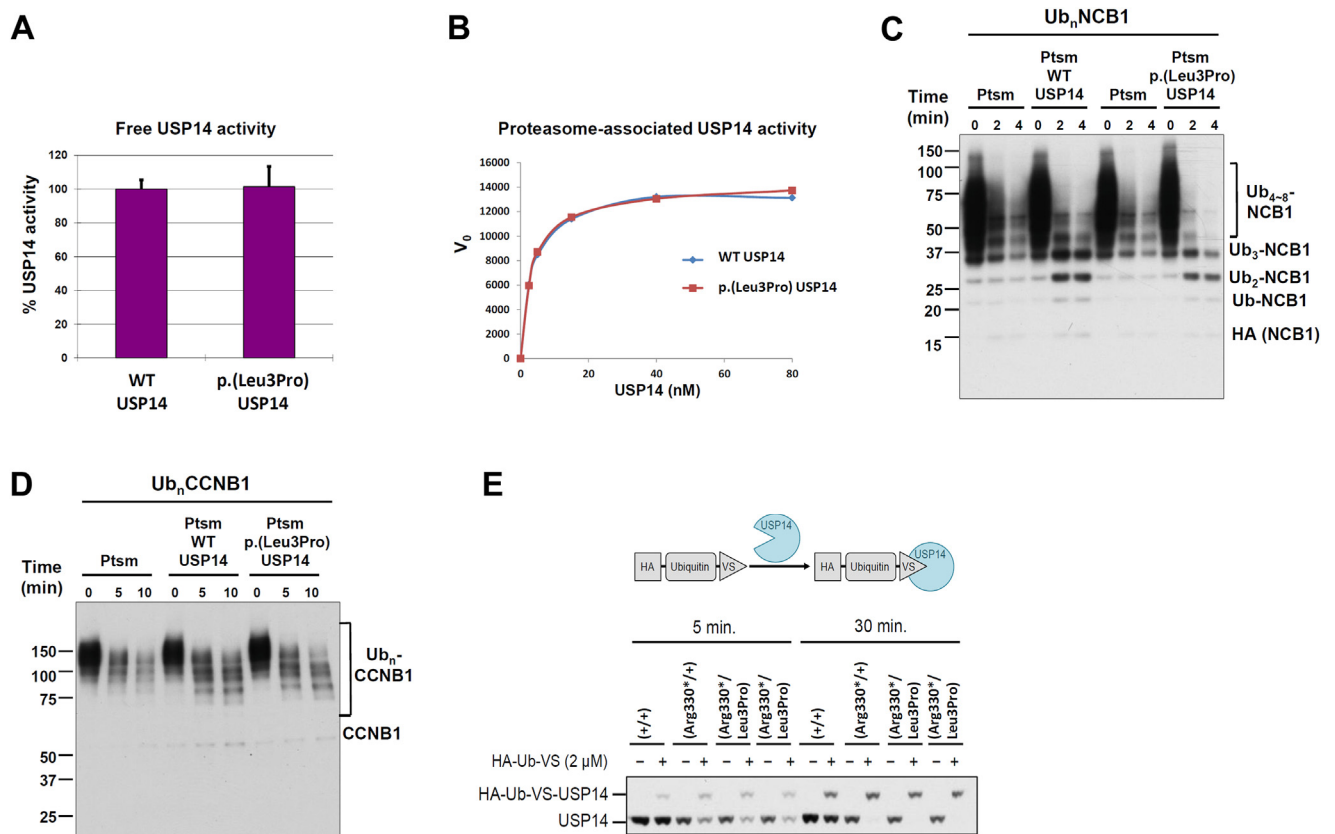
Figure 3   Deubiquitinating activity of recombinant p.(Leu3Pro) USP14. A. Ub-AMC hydrolysis assays with free forms of USP14 WT and p.(Leu3Pro) at 1.5 μM. Error bars represent SD from triplicate experiments. B. Kinetic analysis of proteasome-bound USP14 WT and p.(Leu3Pro) activities with Ub-AMC as substrate. Graded concentrations of recombinant USP14 were reconstituted with 1 nM Ub-VS-treated proteasome, and cleavage of Ub-AMC (1 μM) by USP14 was measured over 80 minutes in real time. The plots shown represent mean values of initial reaction rates from triplicate experiments. C. In vitro deubiquitination/degradation assays with Ub_nNCB1, human proteasome (4 nM), and WT or p.(Leu3Pro) USP14 (80 nM). D. In vitro deubiquitination/degradation assays with Ub_nCCNB1, human proteasome (7 nM), and WT or p.(Leu3Pro) USP14 (140 nM). E. The irreversible covalent modifier ubiquitin vinyl sulfone, carrying an HA epitope tag, was added at 2 μM to lysates from patient fibroblasts, and the samples incubated at 25°C for either 5 or 30 minutes as indicated. Samples were then analyzed by SDS-PAGE and immunoblotting, using an antibody to USP14. Each lane was loaded with 25 μg of lysate. HA-Ub-VS reacts with the catalytic cysteine of proteasome-activated USP14.

Introduction of tagged *USP14* variants into USP14^{−/−} SH-SY5Y cells

We next investigated whether the p.(Arg330*) nonsense variant gives rise to a truncated USP14 protein devoid of active site but still carrying the N-terminal UBL domain required for proteasome binding. Herein, we first generated *USP14* knockout SH-SY5Y cells by a CRISPR/Cas9-based strategy before rescue experiments. As shown in Figure 5A and B, the use of guide RNA targeting the first exon of the *USP14* gene in SH-SY5Y cells efficiently caused nonsense or frameshift variants, which completely abolished USP14 expression in 2 different puromycin-resistant clones (Figure 5C). The loss of *USP14* in these cells was not accompanied by a change of proteasome amounts and/or composition, as evidenced by their Rpt1 and β5 expression levels, which were quite similar to those of the WT SH-SY5Y cell line (Figure 5C). Most importantly, introducing a HIS-tagged version of the p.(Arg330*) variant in USP14^{−/−} clone #16 failed to produce a USP14 truncated protein with

an expected size of 36,7 kDa, as determined by western blotting using antibodies specific for USP14 and HIS (Figure 5D). By contrast, transfection of these cells with HIS-tagged p.(Leu3Pro) USP14 was followed by a parallel rise of USP14, whose expression was, however, much weaker than that of WT USP14 (Figure 5D, Supplemental Figure 5A and B). Importantly, the observed decreased expression of the p.(Leu3Pro) *USP14* variant in these cells did not stem from variations in transfection efficiencies because coadministration of p.(Leu3Pro) USP14 with enhanced green fluorescent protein (EGFP) did not lead to lower EGFP expression levels compared with cells transfected with both WT USP14 and EGFP (Supplemental Figure 5C). On the contrary, EGFP levels were even higher when introduced together with p.(Leu3Pro) USP14 (Supplemental Figure 5C), suggesting a stabilizing effect of this variant on EGFP protein turnover. Altogether, these data indicate that both p.(Arg330*) and p.(Leu3Pro) *USP14* variants negatively affect USP14 steady-state expression in SH-SY5Y cells.
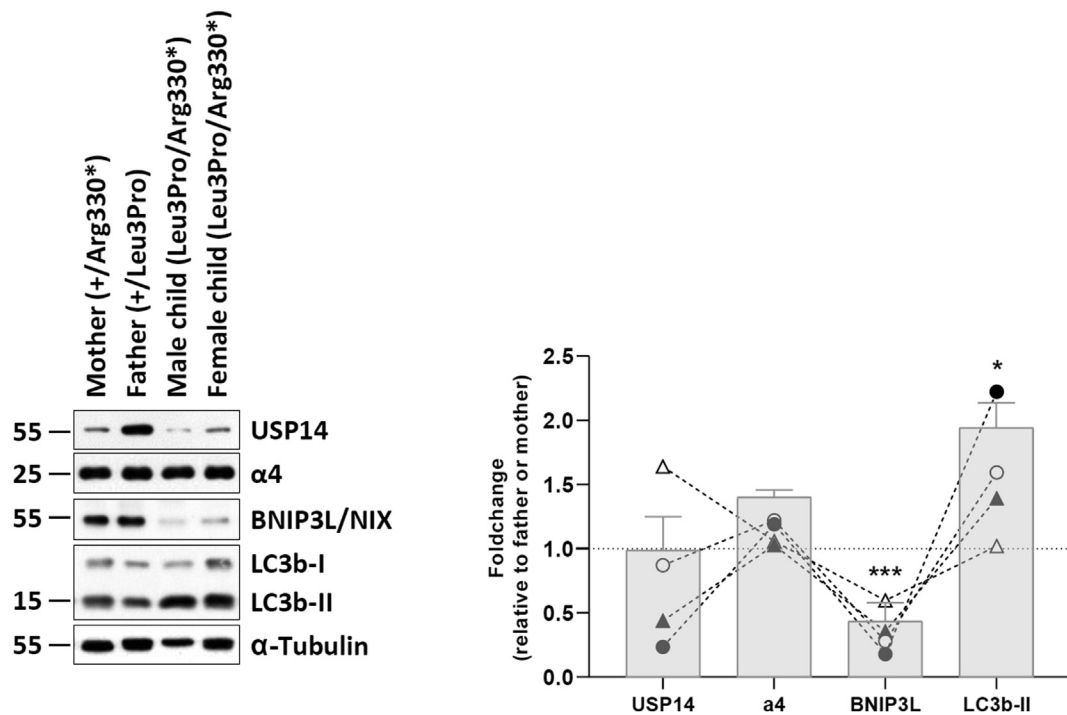
Figure 4   Patients with *UPS14* biallelic variants are associated with alterations of the autophagy/mitophagy pathways. Left panel: 10 to 20 µg of radioimmunoprecipitation assay buffer cell lysates obtained from T cells of subjects with *USP14* variants were separated by SDS-PAGE before western blotting using antibodies specific for USP14, α4, BNIP3L/NIX, LC3B, and α-tubulin (loading control), as indicated. Shown are representative western blots of 3 independent experiments performed. Right panel: Shown is the quantification of the western blots by densitometry. Data are presented as fold changes in the affected male and female children vs their father and/or mother, whose densitometric measurements were set to 1 (gridline), as indicated. Columns indicate the foldchange mean values ± SEM calculated from the normalizations of 3 independent biological replicates. Statistical significance was assessed by unpaired Student's test (*$P < .05$ and ***$P < .001$).

MS analysis of USP14 protein N termini in patient-derived T cells

To further ascertain the impact of the p.(Arg330*) and p.(Leu3Pro) variants on USP14 steady-state expression level, we next conducted a MS analysis of the proteomes from both the siblings and their parents. To this end, whole-cell lysates from primary fibroblasts from 1 unrelated heathy individual and the 4 family members were separated by SDS-PAGE before Coomassie staining. As shown in Figure 6A, gel sections containing the USP14 bands were extracted and subjected to in-gel digestion using trypsin. Interestingly, MS analysis of the resulting products showed that individuals that carry one copy of WT USP14 express 50% (≈20 fmol) of the protein that is found in healthy individual (Figure 6B). As expected, the p.(Leu3Pro) USP14 mutant peptide was only found in individuals carrying the variant (father and both siblings). In line with our western blot analysis (Figure 5D), the p.(Leu3Pro) *USP14* variant was weaker expressed than its WT counterpart (Figure 6B).

Considering the previously documented deleterious effects of proline residues at position +3 on N-terminal methionine excision (NME) of nascent proteins by methionine aminopeptidase (MAP),[29] we next proceeded to investigate whether the p.(Leu3Pro) variant had an impact

on this process. Herein, USP14 immuno-precipitates from primary fibroblast cell lines of all family members were subjected to trypsin digestion before MS analysis. As summarized in Figure 6C, there were no detectable remnants of N-terminal methionine on USP14 peptides derived from the WT allele, suggesting complete N-terminal methionine removal of the newly synthesized USP14 protein under normal conditions. In contrast, a portion of the USP14 p.(Leu3Pro) mutant peptides in all 3 family members harboring this variant retained N-terminal methionine (Figure 6C). These findings suggest that the p.(Leu3Pro) missense variant partially impairs NME of USP14, and this defect appears to be linked to reduced expression of the p.(Leu3Pro) USP14 at the protein level. To further validate this point, we disrupted the accessibility of the N-terminal methionine to MAP by tagging USP14 N-terminally with a double HA epitope. As shown in Supplemental Figure 6, the Leu3Pro substitution had no discernable effect on the steady-state expression of the HA-USP14 fusion protein, confirming that this variant was deleterious only when the initiator methionine is be subjected to NME. Importantly, both c. 233_236del and c. 899_902del *USP14* homozygous deletions identified in P3 and P4 failed to supply stable truncated USP14 proteins in these cells, as determined by western blotting (Supplemental Figure 6). These data
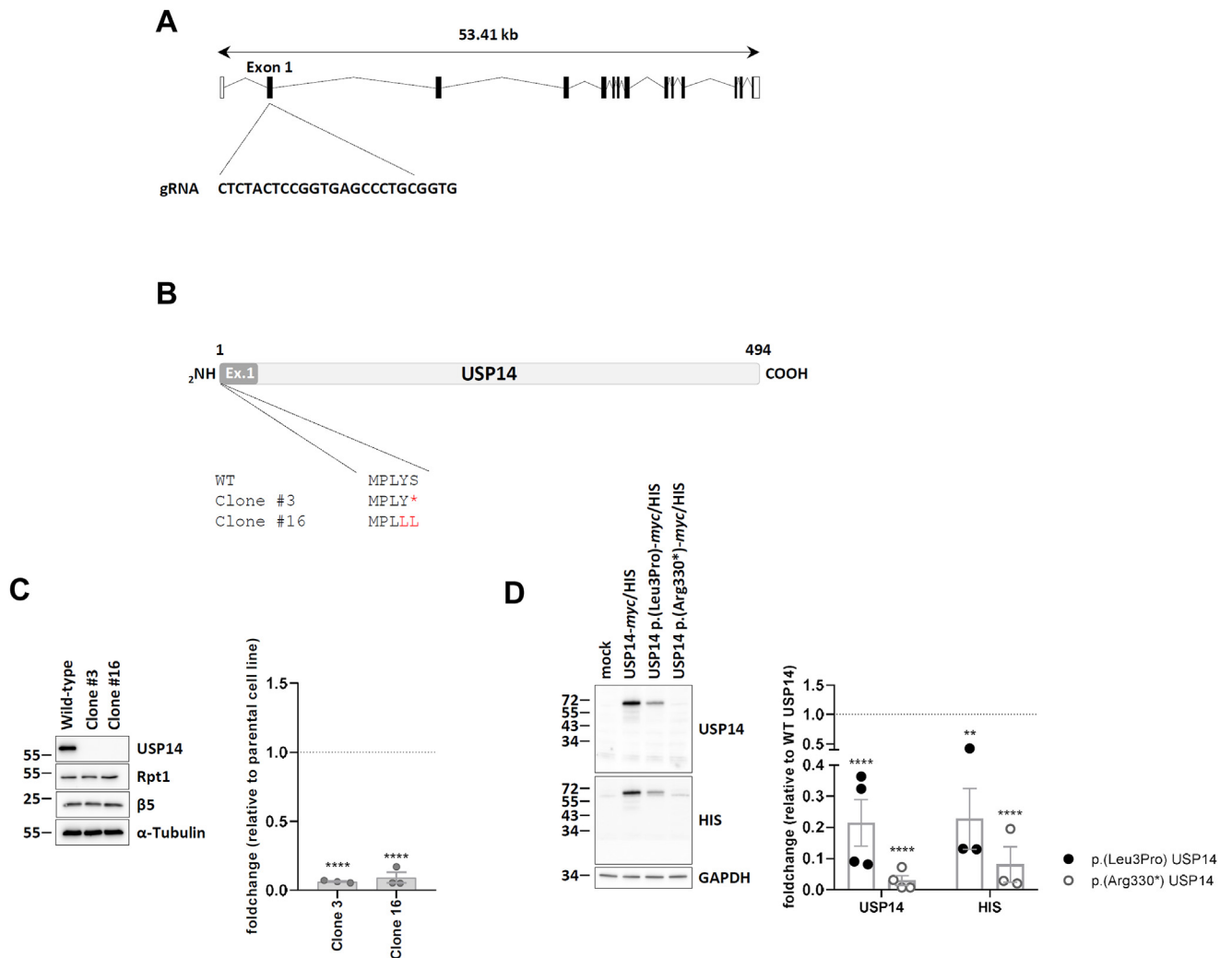
Figure 5 **The p.(Arg330*) nonsense variant fails to give rise to a USP14 truncated variant in USP14−/− SH-SY5Y cells.** A. Schematic representation of the *USP14* gene, as well as the region in exon 1 targeted by the specific guide RNA used for gene deletion by CRISPR/ Cas9. B. Primary structures generated from the sequencing results of *USP14* PCR amplicons obtained for wild-type SHSY-5Y cells and clones #3 and #16, as indicated. C. Left panel: wild-type SHSY-5Y cells and clones #3 and #16 were subjected to SDS-PAGE and western blotting using antibodies specific for USP14, Rpt1, and Beta5, as indicated. Equal protein loading was ensured by using an antibody directed to α-tubulin. Right panel: Shown is the quantification of the western blots by densitometry. Data are presented as fold changes ($n = 3$) in clones #3 and #16 vs the SHSY-5Y parental cell line, whose densitometric measurements were set to 1 (gridline), as indicated. Statistical significance was assessed by unpaired Student's test (****$P < .0001$). D. Left panel: SHSY-5Y clone #16 was subjected to a 24-hour transfection with expression vectors coding for HIS-tagged wild-type UPS14, as well as the p.(Arg330*) or p.(Leu3Pro) USP14 variants. Overexpressed proteins were quantified by SDS-PAGE/western blotting using anti-USP14, anti-HIS, and anti-GAPDH (loading control) antibodies, as indicated. Right panel: Shown is the quantification of the western blots by densitometry. Data are presented as fold changes from at least 3 independent experiments of the USP14 and HIS signals in SHSY-5Y cells transected with the p.(Leu3Pro) (black circles) and p.(Arg330*) (white circles) USP14 variants relative to SHSY-5Y cells transected with wild-type USP14, whose densitometric measurements were set to 1 (gridline), as indicated. Statistical significance was assessed by unpaired Student's test (**$P < .01$ and ****$P < .0001$).

confirm that the 4 *USP14* genomic alterations identified in the 3 families were loss-of-function variants.

Impact of UPS14 dysfunction on type I interferon (IFN) status in patient T cells

Because perturbations of proteasome function typically trigger sterile type I IFN responses in patients,[30] T cells of the 4 family members were next assessed for their content of ISG transcripts using qPCR. As shown in Figure 7, the IFN scores exhibited by the affected female sibling or her parents were not significantly higher than those displayed by any of the 3 healthy donor controls of WT genotype. The male sibling showed a slight increased type I IFN score (Figure 7), which may potentially indicate proteotoxic stress not necessarily related to *USP14* loss of function.
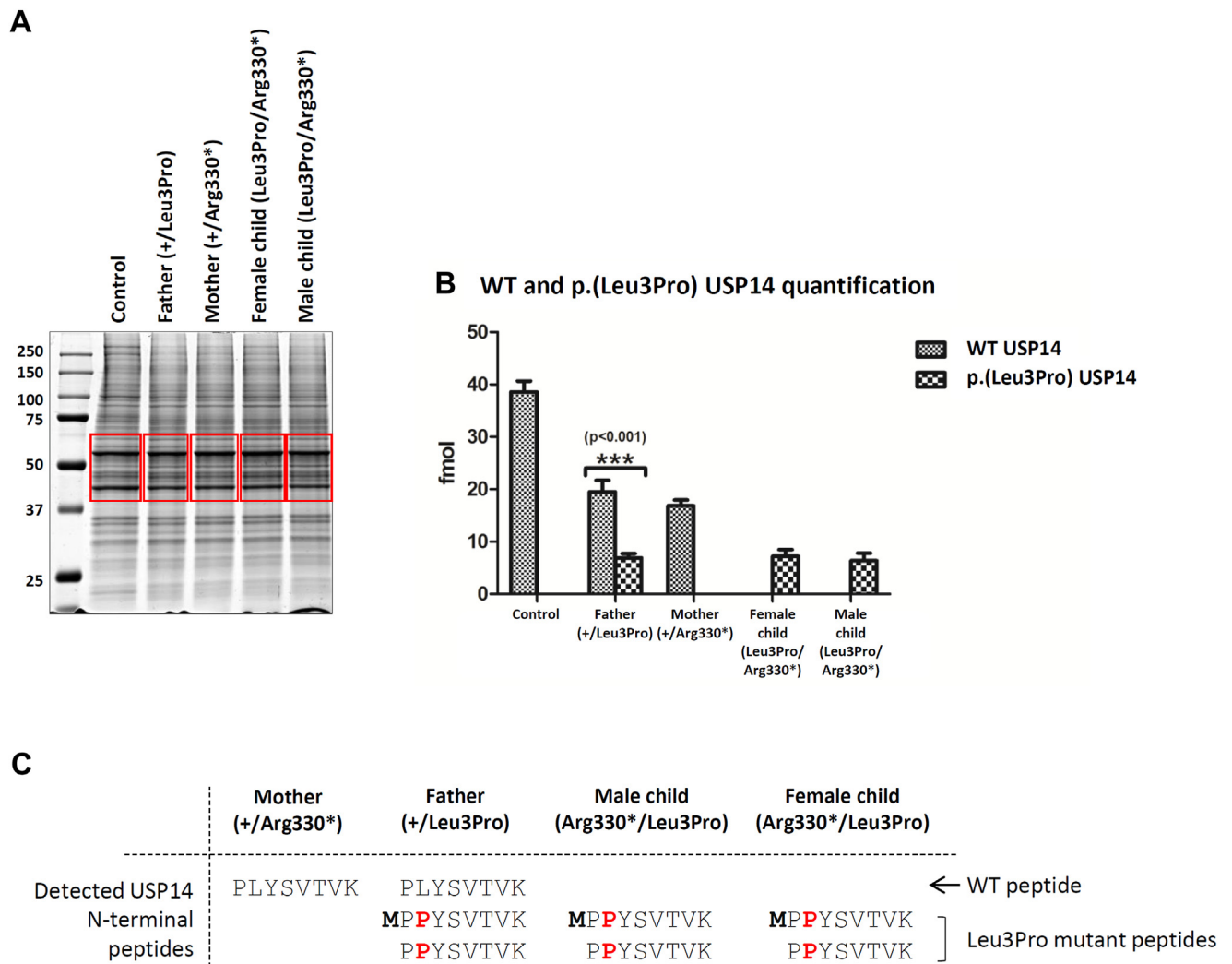
Figure 6 **Mass spectral analysis of whole-cell lysates derived from patient cells reveals decreased expression and N-terminal methionine processing of the p.(Leu3Pro) USP14 variant.** A. Coomassie-stained SDS-PAGE of protein lysates from subjects carrying the p.(Arg330*) and/or p.(Leu3Pro) USP14 variants, as indicated. Gel slices excised for trypsin digestion and subsequent mass spectrometry (MS) analysis are indicated in red. B. Quantification of wild-type (WT) and p.(Leu3Pro) USP14 peptides by MS using a parallel reaction monitoring method. C. Table recapitulating the identification of N-terminal methionine untrimmed and trimmed USP14 WT- and p.(Leu3Pro)-derived peptides found in USP14 immuno-precipitates of each sample, as indicated.

Altogether, these data indicate that both p.(Arg330*) and p.(Leu3Pro) *USP14* variants are deleterious for USP14 function (possibly with some differences with p.(Arg330*) being a complete loss-of-function variant, whereas p.(Leu3Pro) a hypomorphic allele), and their biallelic expression affects autophagy and mitophagy processes without triggering autoinflammation. By adding all these functional studies showing damaging effect on the gene or gene product (American College of Medical Genetics and Genomics criterion PS3), the new classification for p.(Leu3Pro) is likely pathogenic. On the other hand, it was not possible to investigate the functional impact of the 2 frameshift variants because suitable biological samples could not be obtained from individuals 3 and 4.

Discussion

Here, we describe 4 individuals, including a fetal patient, with a phenotypic spectrum involving both neuro-developmental and neuromuscular features caused by *USP14* biallelic pathogenic variants. Recently, the c.233_236del p(.Leu78Glnfs*11) homozygous *USP14* variant has been associated with cerebral malformations with an arthrogryposis multiplex congenita (AMC) phenotype in 3 fetuses from a consanguineous family.[31] In our cohort, individual 3 carrying the c.899_902del p.(Lys300Serfs*24) variant presented with lissencephaly, corpus callosum agenesis, aqueductal stenosis, ventricular dilation, and limbs contractures. Individual 4 carrying the c.233_236del p.(Leu78Glnfs*11) variant at homozygous
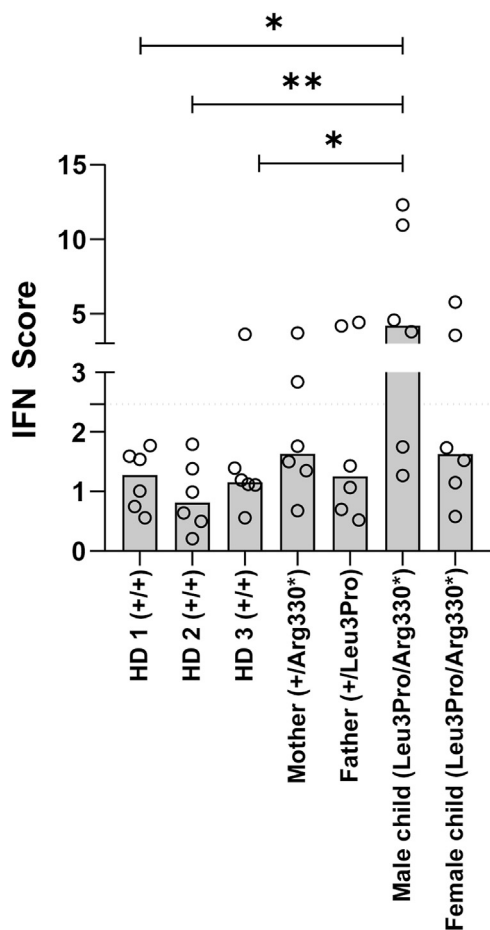
Figure 7 **UPS14 loss-of-function is not consistently associated with sterile type I IFN responses.** Interferon (IFN) scores of whole-blood samples collected and stabilized in PAXgene RNA tubes from 3 unrelated healthy individuals (HD) and subjects carrying the p.(Arg330*) and/or p.(Leu3Pro) USP14 variants, as indicated. Scores were calculated as the median of the relative quantification of 6 ISG (ie, *IFIT1, IFI27, IFI44L, ISG15, RSAD2*, and *SIGLEC1*) over a single calibrator control, as measured by RT-qPCR (see Materials and Methods). Statistical significance was assessed by paired ratio *t* test (*$P < .05$ and **$P < .01$).

state also presented with pachygyria, hydrocephalus, corpus callosum anomalies, and AMC. Introduction of these genomic alterations into SH-SY5Y *USP14$^{-/-}$* cells by plasmid-driven expression failed to generate the corresponding truncated proteins (Supplemental Figure 6), thereby confirming that the 2 biallelic *USP14* deletions were loss-of-function variants associated with CNS malformations.

The 2 individuals carrying compound heterozygous p.(Arg330*) and p.(Leu3Pro) USP14 variants showed a progressive neurological disease (Table 1). Our data revealed that both alterations were associated with reduced USP14 protein expression, although to a much lesser extent for the p.(Leu3Pro) variant (Figures 4-6). Indeed, the 36.7 kDa truncated form of USP14 theoretically produced by p.(Arg330*) variant was not detected in patient-derived

T cells or fibroblasts using SDS-PAGE/western blotting or MS, respectively. Furthermore, this variant could not be ectopically expressed as HIS- or HA-tagged USP14$_{(1-329)}$ fusion protein in USP14$^{-/-}$ SH-SY5Y cells (Figure 5D, Supplemental Figure 6), most likely as a result of a failure of the c.988C>T transcript to escape NMD (Supplemental Figure 2).

Conversely, the p.(Leu3Pro) *USP14* variant was detected at the protein level in patient-derived T cells and fibroblasts. However, its steady-state expression was lower than WT *USP14* (Figures 5D and 6B) and the reduced amounts of p.(Leu3Pro) USP14 were associated with reduced NME (Figure 6C). This observation is fully in line with previous studies showing that NME by MAP is favored by proline residues at position P2—directly after the initiator methionine (P1), but not at P3.[29,32] NME is a highly conserved limited proteolysis process that occurs cotranslationally and whose functional significance remains poorly understood. It has been proposed that NME might serve various functional purposes such as in methionine recycling, PTM, the latter being closely linked to protein folding and/or turnover, particularly through N-terminal acetylation[33] As such, it is tempting to speculate that p.(Leu3Pro) USP14 mutant proteins are less stable than their WT counterparts because of inefficient NME. Supporting this notion, rendering p.(Leu3Pro) USP14 insensitive to NME by tagging it at the N terminus with a double HA epitope led to protein expression levels comparable to those of HA-tagged WT USP14 (Supplemental Figure 6). However, the mechanisms by which perturbed NME alters the turnover of the p.(Leu3Pro) USP14 variant remain unclear because we were unable to rescue its expression following proteasome inhibition (Supplemental Figure 2A and B). These observations suggest that untrimmed p.(Leu3Pro) USP14 may not be targeted for proteasomal degradation or exhibit a half-life longer than the 4-hour bortezomib treatment used in these assays. Another factor contributing to the reduced levels of p.(Leu3Pro) USP14 might be a decreased expression of the corresponding c.8T>C mutant mRNA. Regrettably, quantifying the expression of this transcript by allele-specific RT-qPCR proved challenging because of GC-rich regions surrounding the nucleotide substitution. Interestingly, the p.(Leu3Pro) USP14 variant seemed to exhibit slightly higher activity than WT USP14 in cellulo (Figure 3E), suggesting that aberrant DUB function might participate in the pathogenesis of this variant as well.

Interestingly, to the best of our knowledge, this study represents one of the very few reporting impaired NME as a potential underlying factor in diseases caused by genetic variants. Indeed, aside from a study by Sheikh et al[34] documenting the effects of p.(Ala2Val) variant on methyl CpG-binding protein 2 (MeCP2) NME in Rett syndrome (RTT), our literature research failed to identify any other studies reporting similar pathogenic mechanisms.

In addition to their impact on USP14 protein expression, *USP14* variant exerted effects on proteasomes, whose chymotrypsin-like activity was increased in individuals

carrying single and/or biallelic variants (Figure 2). The downregulation of proteasome activity by USP14 is a well-documented process relying on USP14's UBL domain, which targets USP14 to 26S complexes.[23,35] Because the Leu3Pro substitution is located within the UBL domain of USP14 (Figure 1), it is conceivable that the ability of the resulting variant to activate proteasomes may reflect its inability to associate with them. The observation that WT and p.(Leu3Pro) USP14 reach comparable active states in the presence of purified 26S proteasomes in vitro (Figure 3B) rather suggests that this effect might be due to a reduced availability of USP14 for binding to proteasomes. It is noteworthy that USP14 is subjected to PTM, in particular by the AKT kinase, which phosphorylates Ser432 within the catalytic domain of USP14.[36] Modification at this site has been estimated to enhance the deubiquitinating activity of proteasome-bound USP14 by approximately 2-fold. Whether this modification affects the expressivity of the variants described in this study remains, however, to be determined. Despite exhibiting similar affinities for the proteasome, these forms of USP14 may potentially have distinct effects on ATPase alignment and/or 20S gating mechanisms. In any case, the effects exerted by the p.(Arg330*) or p.(Leu3Pro) monoallelic variants on proteasome activity are unlikely to reach the threshold for disease pathogenesis, because these effects are observed in the T cells from the siblings' parents who are clinically unaffected.

An additional driver of these phenotypes might be a dysregulation of the autophagy and mitophagy processes, which was detected in the T cells from both male and female affected children (Figure 4). The molecular mechanisms by which the combined, but not single, expression of the p.(Arg330*) and p.(Leu3Pro) USP14 variants promote autophagy in patients' T cells are unclear, but this observation is consistent with previous studies showing that USP14 inhibition stimulates autophagosome formation.[37] It is, indeed, argued that UPS14 typically counteracts autophagy by deubiquitinating K63-linked ubiquitin chains from Beclin-1, a process required for activating the vacuolar protein sorting 34 kinase.[38] Whether Beclin-1 ubiquitination is specifically affected by the 2 p.(Arg330*) and p.(Leu3-Pro) USP14 recessive alleles in these patients remains to be formally demonstrated.

Interestingly, recent studies have revealed that the induction of mitophagy by USP14 gene silencing or inhibition can effectively rescue mitochondrial dysfunction in a Drosophila model of Parkinson's disease.[39] Remarkably, this was accompanied by improved locomotion behavior and a notable delay in the progression neurodegeneration. These compelling observations suggest that, although USP14 deficiency is associated with early-onset NDD, it paradoxically exerts beneficial effects in the context of late-onset neurodegenerative diseases. One plausible explanation for these contrasting results is that a major contributing factor of neurodegeneration is a decline in proteasome function, which can be effectively corrected by suppressing USP14, although future studies are needed to fully clarify this point.

All the experimental studies performed indicated that p.(Arg330*) behaves as a nearly complete loss-of-function variant; conversely, the p.(Leu3Pro) variant is possibly a hypomorphic allele, partly affecting some of the USP14 functions. This could explain the different phenotypes observed in the individuals reported in this study: indeed, affected subjects from family 1 (compound heterozygotes for p.(Arg330*) and p.(Leu3Pro)) have a milder clinical presentation compared with the severe phenotype characterizing patients 3 and 4 (who were homozygous for complete loss-of-function variants).

The molecular mechanisms underlying the impact of USP14 loss-of-function variants on the pathogenesis of NDD beyond alterations in proteasome-mediated protein breakdown remain unclear. It is plausible that USP14 deficiency could induce perturbations in CNS function and/or development by influencing the expression of specific regulators, such as PRNP, as previously described.[40] In this regard, subsequent studies are warranted to unravel the proteome of neuronal tissues carrying the p.(Arg330*) and p.(Leu3Pro) biallelic USP14 variants. Surprisingly, unlike other proteasome components,[30] USP14 dysfunction was not associated with spontaneous and sterile type I IFN responses (Figure 7). To the best of our knowledge, this is the first proteasome component for which genomic alterations do not lead to type I IFN gene signatures. This might be attributed to the fact that only a fraction of USP14 is bound to the 26S complex. However, further investigations are required to address this hypothesis.

In conclusion, we describe here the clinical consequences of USP14 biallelic loss-of-function variants and underline the importance of a tight regulation of USP14 for both autophagy and UPS-dependent cellular protein degradation, stressing the crucial role of these degradation pathways in human development.

Data Availability

Acknowledgments

Funding

Author Information

Conceptualization: F.E., X.L., S.K., S.B., E.K., D.G., B.I.; Formal Analysis: all authors; Investigation: F.E., X.L., K.Y.S.H., B.-H.L., M.A.P., J.A.P., B.A.Z., M.W., L.F., V.V., B.T., L.P., H.P., S.K., D.F., D.G., B.I.; Supervision: S.B., E.K., D.G., B.I.; Visualization: F.E., X.L., D.G., B.I.; Writing-original draft: F.E., X.L., B.I.; Writing-review and editing: all authors.

Ethics Declaration

Written informed consent was obtained for use of medical history, genetic testing report, and photographs (if applicable), as approved by the Institutional Review Board of CHU Nantes.

Conflict of Interest

The authors declare no conflicts of interest.

Additional Information

The online version of this article (https://doi.org/10.1016/j.gim.2024.101120) contains supplemental material, which is available to authorized users.

Affiliations

[1]University Medicine Greifswald, Institute of Medical Biochemistry and Molecular Biology, Greifswald, Germany; [2]Nantes Université, CNRS, INSERM, L'Institut du Thorax, Nantes, France; [3]Nantes Université, Service de Génétique Médicale, CHU Nantes, Nantes Cedex 1, France; [4]Dept of Cell Biology, Harvard Medical School, Boston, MA; [5]Instituto de Investigación Sanitaria del Principado de Asturias (ISPA), Oviedo, Spain; [6]Dept of New Biology, Daegu Gyeongbuk Institute of Science and Technology (DGIST), Daegu, Korea; [7]Department of Pediatric Neurosciences, Fondazione IRCCS Istituto Neurologico Carlo Besta, Milan, Italy; [8]Département anatomie et cytologie pathologiques, CHU Toulouse, Toulouse, France; [9]Service de Génétique Médicale, Hôpital Purpan, CHU Toulouse, Toulouse, France; [10]Institute for Human Genetics, University Hospital Muenster, Muenster, Germany; [11]Institute of Human Genetics, School of Medicine, Technical University of Munich, Munich, Germany; [12]Institute of Neurogenomics, Helmholtz Zentrum München, Munich, Germany; [13]Unit of Medical Genetics and Neurogenetics, Fondazione IRCCS Istituto Neurologico Carlo Besta, Milan, Italy; [14]Department of Pathophysiology and Transplantation, University of Milan, Milan, Italy

References

1. Rock KL, Gramm C, Rothstein L, et al. Inhibitors of the proteasome block the degradation of most cell proteins and the generation of peptides presented on MHC class I molecules. *Cell*. 1994;78(5):761-771. http://doi.org/10.1016/s0092-8674(94)90462-6

2. Wilkinson KD. Regulation of ubiquitin-dependent processes by deubiquitinating enzymes. *FASEB J*. 1997;11(14):1245-1256. http://doi.org/10.1096/fasebj.11.14.9409543

3. Borodovsky A, Kessler BM, Casagrande R, Overkleeft HS, Wilkinson KD, Ploegh HL. A novel active site-directed probe specific for deubiquitylating enzymes reveals proteasome association of USP14. *EMBO J*. 2001;20(18):5187-5196. http://doi.org/10.1093/emboj/20.18.5187

4. Li T, Naqvi NI, Yang H, Teo TS. Identification of a 26S proteasome-associated UCH in fission yeast. *Biochem Biophys Res Commun*. 2000;272(1):270-275. http://doi.org/10.1006/bbrc.2000.2767

5. Verma R, Aravind L, Oania R, et al. Role of Rpn11 metalloprotease in deubiquitination and degradation by the 26S proteasome. *Science*. 2002;298(5593):611-615. http://doi.org/10.1126/science.1075898

6. Hanna J, Hathaway NA, Tone Y, et al. Deubiquitinating enzyme Ubp6 functions noncatalytically to delay proteasomal degradation. *Cell*. 2006;127(1):99-111. http://doi.org/10.1016/j.cell.2006.07.038

7. Lappe-Siefke C, Loebrich S, Hevers W, et al. The ataxia (axJ) mutation causes abnormal GABAA receptor turnover in mice. *PLoS Genet*. 2009;5(9):e1000631. http://doi.org/10.1371/journal.pgen.1000631

8. Kim E, Park S, Lee JH, et al. Dual function of USP14 deubiquitinase in cellular proteasomal activity and autophagic flux. *Cell Rep*. 2018;24(3):732-743. http://doi.org/10.1016/j.celrep.2018.06.058

9. DiAntonio A, Haghighi AP, Portman SL, Lee JD, Amaranto AM, Goodman CS. Ubiquitination-dependent mechanisms regulate synaptic growth and function. *Nature*. 2001;412(6845):449-452. http://doi.org/10.1038/35086595

10. Ebstein F, Küry S, Papendorf JJ, Krüger E. Neurodevelopmental disorders (NDD) caused by genomic alterations of the ubiquitin-proteasome system (UPS): the possible contribution of immune dysregulation to disease pathogenesis. *Front Mol Neurosci*. 2021;14:733012. http://doi.org/10.3389/fnmol.2021.733012

11. Fountain MD, Oleson DS, Rech ME, et al. Pathogenic variants in USP7 cause a neurodevelopmental disorder with speech delays, altered

behavior, and neurologic anomalies. *Genet Med*. 2019;21(8):1797-1807. http://doi.org/10.1038/s41436-019-0433-1

12. Homan CC, Kumar R, Nguyen LS, et al. Mutations in USP9X are associated with X-linked intellectual disability and disrupt neuronal cell migration and growth. *Am J Hum Genet*. 2014;94(3):470-478. http://doi.org/10.1016/j.ajhg.2014.02.004

13. Hu H, Haas SA, Chelly J, et al. X-exome sequencing of 405 unresolved families identifies seven novel intellectual disability genes. *Mol Psychiatry*. 2016;21(1):133-148. http://doi.org/10.1038/mp.2014.193

14. Jolly LA, Parnell E, Gardner AE, et al. Missense variant contribution to USP9X-female syndrome. *NPJ Genom Med*. 2020;5(1):53. http://doi.org/10.1038/s41525-020-00162-9

15. Martin HC, Jones WD, McIntyre R, et al. Quantifying the contribution of recessive coding variation to developmental disorders. *Science*. 2018;362(6419):1161-1164. http://doi.org/10.1126/science.aar6731

16. McDonell LM, Mirzaa GM, Alcantara D, et al. Mutations in STAMBP, encoding a deubiquitinating enzyme, cause microcephaly-capillary malformation syndrome. *Nat Genet*. 2013;45(5):556-562. http://doi.org/10.1038/ng.2602

17. Ng BG, Eklund EA, Shiryaev SA, et al. Predominant and novel de novo variants in 29 individuals with ALG13 deficiency: clinical description, biomarker status, biochemical analysis, and treatment suggestions. *J Inherit Metab Dis*. 2020;43(6):1333-1348. http://doi.org/10.1002/jimd.12290

18. Santiago-Sim T, Burrage LC, Ebstein F, et al. Biallelic variants in OTUD6B cause an intellectual disability syndrome associated with seizures and dysmorphic features. *Am J Hum Genet*. 2017;100(4):676-688. http://doi.org/10.1016/j.ajhg.2017.03.001

19. Tsai Y, Xia C, Sun Z. The inhibitory effect of 6-gingerol on ubiquitin-specific peptidase 14 enhances autophagy-dependent ferroptosis and anti-tumor *in vivo and in vitro*. *Front Pharmacol*. 2020;11:598555. http://doi.org/10.3389/fphar.2020.598555

20. Gerber SA, Rush J, Stemman O, Kirschner MW, Gygi SP. Absolute quantification of proteins and phosphoproteins from cell lysates by tandem MS. *Proc Natl Acad Sci U S A*. 2003;100(12):6940-6945. http://doi.org/10.1073/pnas.0832254100

21. Sobreira N, Schiettecatte F, Valle D, Hamosh A. GeneMatcher: a matching tool for connecting investigators with an interest in the same gene. *Hum Mutat*. 2015;36(10):928-930. http://doi.org/10.1002/humu.22844

22. Lek M, Karczewski KJ, Minikel EV, et al. Analysis of protein-coding genetic variation in 60,706 humans. *Nature*. 2016;536(7616):285-291. http://doi.org/10.1038/nature19057

23. Wang F, Ning S, Yu B, Wang Y. USP14: structure, function, and target inhibition. *Front Pharmacol*. 2021;12:801328. http://doi.org/10.3389/fphar.2021.801328

24. Richards S, Aziz N, Bale S, et al. Standards and guidelines for the interpretation of sequence variants: a joint consensus recommendation of the American College of Medical Genetics and Genomics and the Association for Molecular Pathology. *Genet Med*. 2015;17(5):405-424. http://doi.org/10.1038/gim.2015.30

25. Küry S, Besnard T, Ebstein F, et al. De novo disruption of the proteasome regulatory subunit PSMD12 causes a syndromic neurodevelopmental disorder. *Am J Hum Genet*. 2017;100(2):352-363. http://doi.org/10.1016/j.ajhg.2017.01.003

26. Kim HT, Goldberg AL. The deubiquitinating enzyme Usp14 allosterically inhibits multiple proteasomal activities and ubiquitin-independent proteolysis. *J Biol Chem*. 2017;292(23):9830-9839. http://doi.org/10.1074/jbc.M116.763128

27. Butt TR, Edavettal SC, Hall JP, Mattern MR. SUMO fusion technology for difficult-to-express proteins. *Protein Expr Purif*. 2005;43(1):1-9. http://doi.org/10.1016/j.pep.2005.03.016

28. Lee BH, Lee MJ, Park S, et al. Enhancement of proteasome activity by a small-molecule inhibitor of USP14. *Nature*. 2010;467(7312):179-184. http://doi.org/10.1038/nature09299

29. Boissel JP, Kasper TJ, Shah SC, Malone JI, Bunn HF. Amino-terminal processing of proteins: hemoglobin South Florida, a variant with retention of initiator methionine and N alpha-acetylation. *Proc Natl Acad Sci U S A*. 1985;82(24):8448-8452. http://doi.org/10.1073/pnas.82.24.8448

30. Papendorf JJ, Krüger E, Ebstein F. Proteostasis perturbations and their roles in causing sterile inflammation and autoinflammatory diseases. *Cells*. 2022;11(9):1422. http://doi.org/10.3390/cells11091422

31. Turgut GT, Altunoglu U, Sivrikoz TS, et al. Functional loss of ubiquitin-specific protease 14 may lead to a novel distal arthrogryposis phenotype. *Clin Genet*. 2022;101(4):421-428. http://doi.org/10.1111/cge.14117

32. Flinta C, Persson B, Jörnvall H, von Heijne G. Sequence determinants of cytosolic N-terminal protein processing. *Eur J Biochem*. 1986;154(1):193-196. http://doi.org/10.1111/j.1432-1033.1986.tb09378.x

33. Ree R, Varland S, Arnesen T. Spotlight on protein N-terminal acetylation. *Exp Mol Med*. 2018;50(7):1-13. http://doi.org/10.1038/s12276-018-0116-z

34. Sheikh TI, de Paz AM, Akhtar S, Ausió J, Vincent JB. MeCP2_E1 N-terminal modifications affect its degradation rate and are disrupted by the Ala2Val Rett mutation. *Hum Mol Genet*. 2017;26(21):4132-4141. http://doi.org/10.1093/hmg/ddx300

35. Shin JY, Muniyappan S, Tran NN, Park H, Lee SB, Lee BH. Deubiquitination reactions on the proteasome for proteasome versatility. *Int J Mol Sci*. 2020;21(15):5312. http://doi.org/10.3390/ijms21155312

36. Xu D, Shan B, Lee BH, et al. Phosphorylation and activation of ubiquitin-specific protease-14 by Akt regulates the ubiquitin-proteasome system. *Elife*. 2015;4:e10510. http://doi.org/10.7554/eLife.10510

37. Xu D, Shan B, Sun H, et al. USP14 regulates autophagy by suppressing K63 ubiquitination of Beclin 1. *Genes Dev*. 2016;30(15):1718-1730. http://doi.org/10.1101/gad.285122.116

38. Xia P, Wang S, Du Y, et al. WASH inhibits autophagy through suppression of Beclin 1 ubiquitination. *EMBO J*. 2013;32(20):2685-2696. http://doi.org/10.1038/emboj.2013.189

39. Chakraborty J, von Stockum S, Marchesan E, et al. USP14 inhibition corrects an *in vivo* model of impaired mitophagy. *EMBO Mol Med*. 2018;10(11):e9014. http://doi.org/10.15252/emmm.201809014

40. Tian T, McLean JW, Wilson JA, Wilson SM. Examination of genetic and pharmacological tools to study the proteasomal deubiquitinating enzyme ubiquitin-specific protease 14 in the nervous system. *J Neurochem*. 2021;156(3):309-323. http://doi.org/10.1111/jnc.15180